# High Efficiency and Triple-Band Metamaterial Electromagnetic Energy Hervester

S. D. Assimonis[1], T. Kollatou[2], D. Tsiamitros[2], D. Stimoniaris[2], T. Samaras[1], and J. N. Sahalos[1,3]

[1] School of Physics, Aristotle University of Thessaloniki, Greece
assimonis@physics.auth.gr, theosama@auth.gr
[2] Dept. of Electrical Engineering, TEI of Western Macedonia, Kozani, Greece
tkollatou@gmail.com, dtsiamitros@gmail.com, dstimoniaris@yahoo.gr
[3] Dept. of Electrical & Computer Engineering, University of Nicosia, Cyprus
sahalos@auth.gr

## Abstract

**This work describes and proposes a new triple-band (GSM 900, DCS 1800, WiFi), highly efficient metamaterial harvester that is capable to operate in wide angles of plane wave incidence. The energy harvesting structure consists of a conventional metamaterial electric resonator, which employs a via that channels all the absorbed RF power to a resistive load. The latter represents the input impendance of a RF-to-DC rectifier. The metamaterial harvester is analyzed in terms of absorbance, power efficiency and power losses mechanism for normal as well as for wide angle incidence. The assets of the proposed model, could be proven to be potentially instructive for various electromagnetic RF energy harvesting configurations.**

## 1. Introduction

Metamaterials certainly represent one of the most recent research achievements in the field of unconventional materials and complex media. They are expected to have an impact across the entire range of technologies where electromagnetic radiation is used. One very common definition considers metamaterials as artificially engineered, subwavelength structures that exhibit unique electromagnetic properties not readily observed in nature at the frequencies of interest and, thus, allow going beyond some of the limitations encountered when using natural materials in microwave and optical components [1]. Actually, these unusual, exotic features have inspired several applications in various engineering fields, like antennas, substrates, cloaking, and shielding, to name only a few [2, 3].

Although initial interest in metamaterials arose due to their unique electromagnetic effects they have been proven to be excellent candidates for electromagnetic wave absorbers. A particular branch of metamaterial absorbers – the metamaterial perfect absorber (MPA) – has become the main focus due to its ability to offer near unity absorption of electromagnetic waves. In fact, although the first experimental results on metamaterial perfect absorbers were in the microwave frequency realm [4] work quickly followed in the THz and even visible frequencies [5, 6]. A typical MPA's unit cell consists of an imprinted metallic resonating structure on the front side of a dielectric spacer backed by a ground plane. In theory, in order to maximize the absorption rate, we can minimize the reflection and transmission simultaneously at the same frequency range. The reflection can be minimized by tuning the metamaterial impedance equal to one, and hence, becomes matched to the free space.

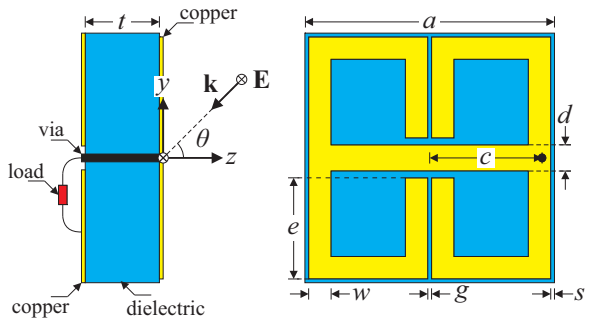


**Figure 1.** The unit cell schematic of the proposed metamaterial harvester: it is a conventional electric resonator with a resistor loaded in a specific position. Plane wave impinges with $\theta$ angle of incidence, while electric component always perpendicular to the $zy$-plane

**Table 1.** The meta-harvester unit cell dimensions (mm)

| $a$ | $c$ | $d$ | $e$ | $g$ | $s$ | $w$ | $t$ |
|---|---|---|---|---|---|---|---|
| 33.31 | 15 | 3.5 | 13.5 | 0.5 | 0.5 | 3 | 9.9 |

A critical difference between a typical metamaterial absorber (*meta-absorber*) and a metamaterial harvester (*meta-harvester*) is that while in the first case the captured power mainly dissipates in the dielectric substrate and the metallic parts, in the second case, the captured power is mainly delivered to a properly placed load, which represents the input impedance of a rectification circuit [7–10]. A typical structure of meta-harvesters can outperform a conventional rectification system [11, 12], which consists of an antenna and a rectifier (i.e. rectenna), to the following: in general, metamaterials are periodic structures, and a typical metamaterial's unit-cell size is $\lambda/10$. Hence, a meta-harvester could be used on grids (similar to photovoltaic panels) and consequently capture more energy and at the same time operate at low frequency bands (e.g. FM radio, digital TV), and carry more power.

The purpose of this paper is to present the design of a new, triple-band (GSM 900, DCS 1800, WiFi), highly-efficient, wide-angle meta-harvester. The design is based on an array of

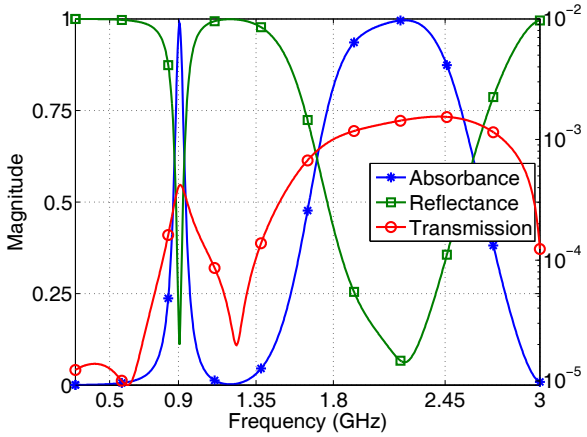


**Figure 2.** Simulated absorbance and reflectance for normal incidence are plotted from zero to one on the left axis, while transmission is plotted from $10^{-5}$ to $10^{-2}$ on the right axis. Perfect Absorbance (100%) occurs at 0.9 and 2.2 GHz, while is well above 80% at 1.8 and 2.45 GHz

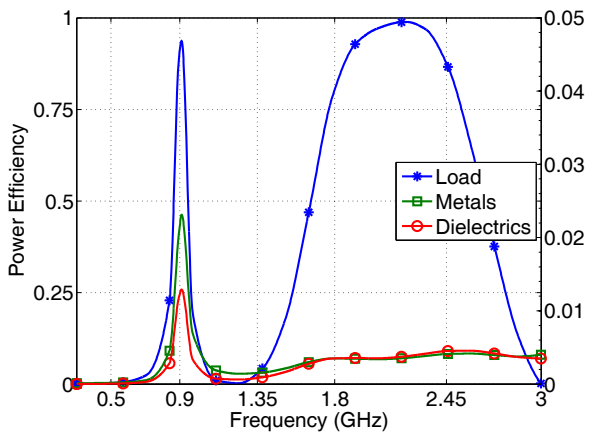


**Figure 3.** Simulated power efficiency at load (left axis). Over 94% and 98% of the incident power is delivered to the load at 0.9 and 2.2 GHz, respectively, while for 1.8 and 2.45 GHz the load captures 81% and 87% of the incident power. It is also plotted (right axis) the power efficiency on dielectric and metallic parts: it is observed that the absorbed power is mainly dissipated to the load

square type ELC (Electric-Inductive-Capacitive) resonators that are capable of high absorption. By incorporating a resistive load in the structure and after a proper design, the meta-absorber is converted to a meta-harvester and almost all the absorbed power is driven to the load. A full length electromagnetic analysis, through simulation results, is carried out unveiling the wide-angle character of the structure as well as it's highly absorptive feature.

## 2. Metamaterial Harvester

The absorbing properties of a meta-harvester depend on the electromagnetic characteristics of the dielectric substrate along with the metallization geometry of the unit-cell and the load (location and resistance). In order to minimize the losses at dielectric, foam with a relative permittivity $\epsilon_r = 1.04$, loss tangent $\tan\delta = 0.001$ and thickness $t = 9.9$ mm is chosen as the substrate for the proposed structure, which is presented in Fig. 1. All the metallic parts are made of copper with thickness 35 $\mu$m, which introduces metallic losses. A conventional ELC resonator [13] is imprinted on the front face of the dielectric spacer whereas the bottom layer is a full copper plane that minimizes the transmission through the slab. The unit-cell dimension and periodicity is around $\lambda/10$, where $\lambda$ is the wavenumber at 0.9 GHz. The resonance frequency can be altered by tuning the gaps and other geometric features of the resonator, depending on the desired operation frequency spectrum.

The main difference between the proposed design and a conventional electric resonator is a carefully placed via that connects a resistive load between the top and bottom conductive layers. Through this via, the induced electric surface currents are driven to a 50 $\Omega$ resistive load, which can be accounted for an input impedance of a typical rectification RF-to-DC system [11, 12].

An array of infinite unit cells is formed by applying periodic boundary conditions along the $x$- and $y$-axis, while at $z$-axis Floquet boundary conditions were applied. The chosen transmitted mode corresponds to a plane wave with the electric component perpendicular to $zy$-plane. All simulations are carried out using the the electromagnetic full-wave simulator ANSYS® HFSS™. In order to design the meta-harvester unit-cell, an optimization procedure was applied. The goal was the maximization of the unit cell *absorbance*,

$$A(\omega) = 1 - |S_{11}|^2 - |S_{21}|^2 \tag{1}$$

where, $S_{11}$ and $S_{21}$ is the reflectance and transmission coefficient, respectively, and simultaneously, the maximization of the unit-cell *power efficiency* at load,

$$\eta = \frac{P_{\rm L}}{P_{\rm inc}} \tag{2}$$

where, $P_{\rm L}$ is the delivered to the load power and $P_{\rm inc}$ is the incident to the meta-harvester power. Similarly, is defined the power efficiency at dielectric substrate and metals as the ratio

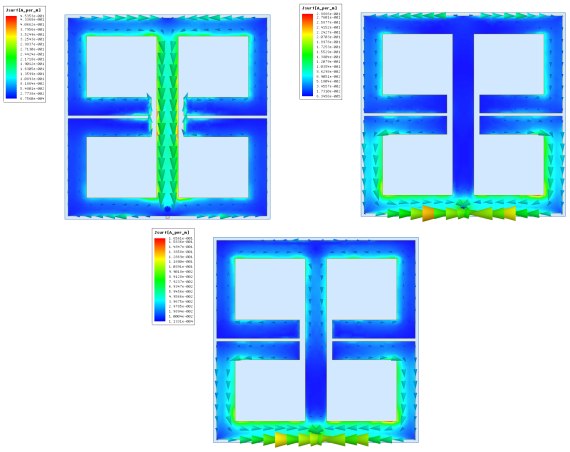

**Figure 4.** Surface current distributions on the front side of the triple-band meta-harvester at the three resonating frequencies 0.9 GHz (top, left), 1.8 GHz (top, right) and 2.45 GHz (bottom, center).

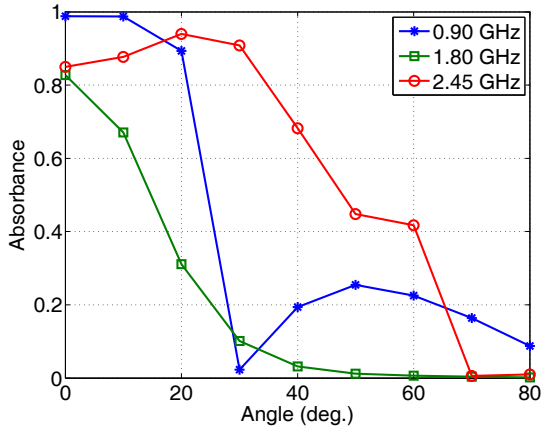


**Figure 5.** The simulated absorbance of the proposed meta-harvester for obliquely incident plane wave at 0.9, 1.8 and 2.45 GHz. It is observed that, meta-harvester absorbs power with high efficiency for a wide-angle variation at all frequency cases

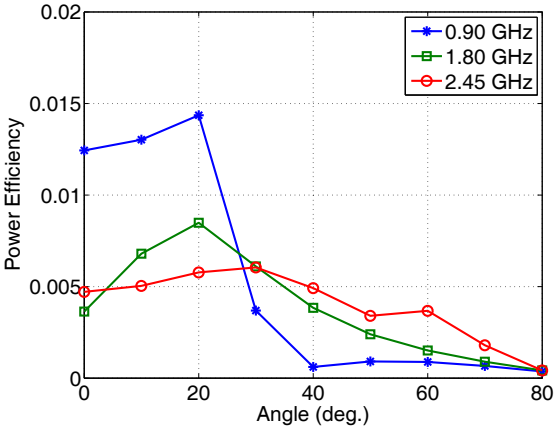


**Figure 7.** The simulated power efficiency on dielectric parts for obliquely incident plane wave at 0.9, 1.8 and 2.45 GHz. It is observed that, the dielectric losses is constantly below 1.5% of the incident power

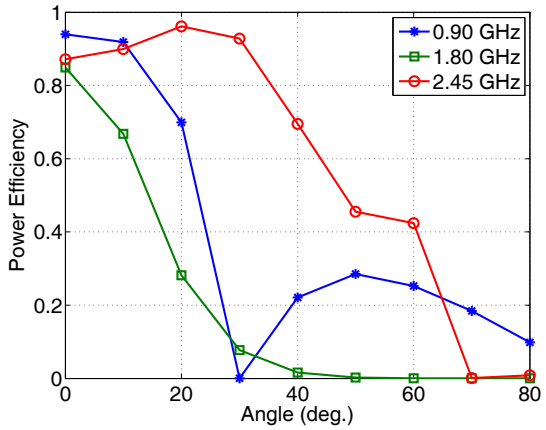


**Figure 6.** The simulated meta-harvester power efficiency at load for obliquely incident plane wave at 0.9, 1.8 and 2.45 GHz. It is observed that meta-harvester delivers power to the load with high efficiency for a wide-angle variation at all cases

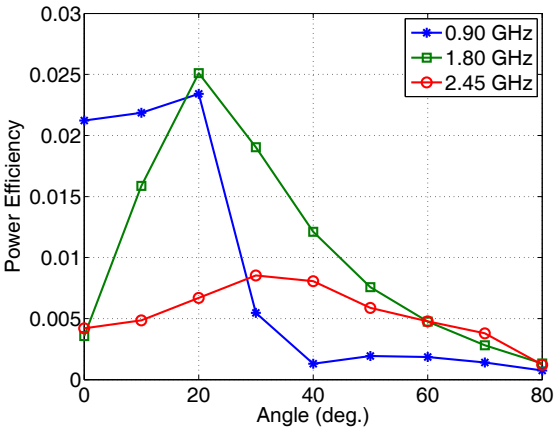


**Figure 8.** The simulated power efficiency on metallic parts for obliquely incident plane wave at 0.9, 1.8 and 2.45 GHz. It is observed that, the metallic losses is constantly below 2.5% of the incident power

$P_{\rm dlc}/P_{\rm inc}$ and $P_{\rm mtl}/P_{\rm inc}$, respectively, where $P_{\rm dlc}$ and $P_{\rm mtl}$ are the dissipated power on dielectric and metallic parts, respectively. The degrees of freedom were the dimensions (Fig. 1) $c$, $d$, $e$, $g$, $s$, and $w$, while $a$ and load resistance was fixed at $\lambda/10$ and 50 $\Omega$, respectively. After simulation, the obtained metamaterial unit cell dimensions are tabulated in Table 1.

Simulated results for absorbance and reflectance at the case of normal incidence are plotted from zero to one on the left axis, while transmission is plotted from $10^{-5}$ to $10^{-2}$ on the right axis in Fig. 2. The first and the second perfect absorption peak of 100% occurs at the frequency of 0.9 and 2.2 GHz, respectively, while the reflectance is minimized at the same frequency. More specific, the high absorptive region remains above 80% for $0.8876-0.9234$ GHz and for $1.7915-2.5129$ GHz. Hence, the meta-harvester could capture RF energy from GSM 900, DCS 1800 and WiFi frequency bands.

The simulated power efficiency at is depicted in Fig. 3 (left axis). Over 94% and 98% of the incident power is delivered to the load at 0.9 and 2.2 GHz, respectively, while for 1.8 and 2.45 GHz the load captures 81% and 87%, of the incident power, respectively, enhancing the characterization of our structure as an efficient meta-harvester. On the other hand, power efficiency on dielectric and metallic parts remains constantly bellow 2.5% (Fig. 3, right axis).

The absorption mechanism is an issue of careful investigation, since it offers a valuable physical insight to the problem under analysis. In a typical meta-absorber, there are two possible loss mechanisms that are generally accepted in the literature; dielectric losses arising from the imaginary part of the substrate's dielectric constant and metallic losses due to the imperfect conductivity of the metallic parts of the structure. In order to have high absorption, dielectric with high losses is desired. On the other hand, on a meta-harvester, dielectric and metallic losses should be minimized, while power delivered to the load should be maximized. In this case (Fig. 3), it is obvious that the power distribution within the unit cell in high absorp-

tion is significantly affected by the implanted via that drives the power towards the load.

Additionally, in order to enhance the aforementioned observations and gain an insight into the physical resonant behavior mechanism of the device, the surface current distributions at the three resonant frequencies are illustrated in Fig. 4. Evidently, the current flows towards the via in all the three cases of resonance. At $0.9$ GHz, the current is flowing through the middle metallic part while in the other two resonant frequencies $1.8$ GHz and $2.45$ GHz, the peripheral flow of the current is apparent. The surface current on the two rings generates anti-circulating currents that merge at the bottom of the cell where the via is strategically placed to allow the maximum current flow to the load.

Next, an elaborated analysis is also conducted on the wide angle performance of the proposed structure, proving its efficient operation for the various scenarios of oblique incidence. By retaining the electric field component perpendicular to the $zy$-plane we modify the angle $\theta$, between the wavevector $\mathbf{k}$ and the $z$-axis, where $0^\circ \leq \theta \leq 80^\circ$. It is noted that the geometry is symmetrical at $zx$-plane. The simulated results at $0.9$, $1.8$ and $2.45$ GHz are depicted in Fig. 5. The first observation concerns the absorption for the first resonant frequency of $0.9$ GHz. The meta-harvester perfectly captures RF power from $-10^\circ$ to $+10^\circ$. The absorbance is constantly over $80\%$ from $-25^\circ$ to $+25^\circ$, while at $30^\circ$ there is a critical drop. At $1.8$ GHz, the absorption deteriorates beyond $65\%$ for $|\theta| \geq 10^\circ$. Finally, at $2.45$ GHz the absorbance remains above $40\%$ for a variation of $-60^\circ \leq \theta \leq 60^\circ$, a very good result for a wide angle absorber at WiFi frequency band.

Fig. 6 depicts the meta-harvester simulated power efficiency at load for obliquely incident plane wave at $0.9$, $1.8$ and $2.45$ GHz. Results are similar with Fig. 5: at all cases, the proposed meta-harvester delivers power to the load with high efficiency for a wide-angle variation. Especially at $2.45$ GHz power efficiency remains constantly over $40\%$ for $-60^\circ \leq \theta \leq 60^\circ$.

Finally, Fig. 7 and 8 depict the simulated power efficiency on dielectric substrate and metallic parts, respectively, for obliquely incident plane wave at the three resonance frequencies. It is observed than the dielectric and metallic losses is constantly below $1.5\%$ and $2.5\%$ of the incident power, respectively. Consequently, it is evident that for the power absorption the load plays the major part.

## 3. Conclusion

In this paper, the design and simulation of a novel optimized meta-harvester with the ability to achieve high efficiency, triple-band absorption and drive almost all the absorbed power to a resistive load has been demonstrated. A thorough investigation has been performed and presented to better understand the physical mechanism of the power distribution for normal and oblique incidence. The promising absorbing and power harvesting performance of the proposed design renders the structure appropriate not only on RF power harvesting systems but also on wireless power transfer systems.

## 4. References


[1] R. Marqués, F. Martín, and M. Sorolla, "Metamaterials with Negative Parameters: Theory, Design, and Microwave Applications," *John Wiley & Sons*, New York, 2008.

[2] F. Bilotti, S. Tricarico, and L. Vegni, "Plasmonic Metamaterial Cloaking at Optical Frequencies," *IEEE Trans. Nanotechnol.*, vol. 9, no. 1, pp: 55–61, 2009.

[3] M. Veysi, M. Kamyab, J. Moghaddasi, and A. Jafargholi, "Transmission phase characterizations of metamaterial covers for antenna application," *Prog. Electromagn. Res. Lett.*, vol. 21, pp: 49–57, 2011.

[4] N. Y. Landy, S. Sajuyigbe, J. J. Mock, D. R. Smith, and W. J. Padilla, "Perfect metamaterial absorber," *Phys. Rev. Lett.*, vol. 100, 207402, 2008.

[5] C. M. Watts, X. Liu, and W. J. Padilla "Metamaterial Electromagnetic Wave Absorbers," *Adv. Mater.*, 24(23), OP98–OP120, 2012.

[6] H. Tao, C. Bingham, A. Strikwerda, D. Pilon, D. Shrekenhamer, N. Landy, K. Fan, X. Zhang, W. Padila, and R. Averitt, "Highly flexible wide angle of incidence terahertz metamaterial absorber: Design, fabrication and characterization," *Phys. Rev. B*, vol. 78, no. 24, pp. 241103(1–4), 2008.

[7] O. M. Ramahi, T. S. Almoneef, M. Alshareef, and M. S. Boybay, "Metamaterial particles for electromagnetic energy harvesting," *Appl. Phys. Lett.*, 101, 173903–173903 (2012).

[8] T. Almoneef and O. M. Ramahi, "A 3-dimensional stacked metamaterial arrays for electromagnetic energy harvesting," *Prog. In Electromagn. Res.*, vol. 146, pp. 109–115, 2014.

[9] B. Alavikia, T. S. Almoneef, and O. M. Ramahi, "Electromagnetic energy harvesting using complementary split-ring resonators," *Appl. Phys. Lett.*, 104, 163903, 2014.

[10] T. S. Almoneef, and O. M. Ramahi, "Metamaterial electromagnetic energy harvester with near unity efficiency," *Appl. Phys. Lett.*, 106, 153902, 2015.

[11] A. Georgiadis, G. Andia, and A. Collado, "Rectenna design and optimization using reciprocity theory and harmonic balance analysis for electromagnetic (EM) energy harvesting," *IEEE Antennas Wireless Propag. Lett.*, vol. 9, pp. 444–446, 2010.

[12] S. D. Assimonis, S.-N. Daskalakis, and A. Bletsas, "Efficient RF harvesting for low-power input with low-cost lossy substrate rectenna grid," in *Proc. IEEE Int. RFID-Technol. Appl. Conf.*, Tampere, Finland, Sept. 2014.

[13] H. T. Chen, J. F. O'Hara, A. J. Taylor, R. D. Averitt, C. Highstrete, M. Lee, and W. J. Padilla, "Complementary planar terahertz metamaterials," *Opt. Express.*, vol. 15, pp. 1084–1095, 2007.